Seismic-Resistance Performance Evaluation and Strengthening Effect of Reinforced Concrete Moment Frame

K. J. Shin, D. B. Kim, H. D. Lee & S. H. Lee
Kyungpook National University, Republic of Korea

15 WCEE
LISBOA 2012

SUMMARY: Design requirements for an earthquake-resistant structure are determined by the seismic design category (SDC). In general, SDC relates to considerations of seismic hazard level, soil type, occupancy, and use of the building. The seismic-force-resisting system is divided into three types of moment frame, ordinary moment frame (OMF), intermediate moment frame (IMF), and special moment frame (SMF), according to sections to be satisfied in SDC. In this study three reinforced concrete frames of an OMF with non-seismic provision and two IMFs designed mainly for gravity loads according to the Korean Building Code 2009 were prepared. And three specimens of OMF, IMF and IMF strengthening with carbon fiber reinforced polymer (CFRP) were tested under static reversed cyclic loading according to ACI 374.1-05 to simulate the seismic-type forces. The test results shows that the CFRP reinforcing increases the load carrying capacity of IMF, but the strengthening effect is not large enough than expected.

Keywords: seismic design category, ordinary moment frame, intermediate moment frame, cyclic loading

1. INTRODUCTION

Earthquakes have been increasing recently all over the world with more detrimental damage. In the past three years, Turkey, Haiti, Chile, and Japan have suffered from earthquakes of Richter scale of 6.0, 7.0, 8.8, and 9.1, respectively, and the economic damage and human life loss are very arduous. Most of the old low-rise concrete buildings have been built without seismic-resistant provision and reinforcing of old structure is required for the future seismic. Many studies on seismic-resistant technology have been performed over and over for decades. In ACI-318, earthquake-resistant moment frames are classified into three groups, ordinary moment frame (OMF), intermediate moment frame (IMF), and special moment frame (SMF), that will be placed in areas of seismic risk and seismic design category (SDC). The performance of the column member between OMF and IMF was compared (Han et al. 2005). An experimental study on effectiveness of FRP wraps in controlling the location of a Plastic Hinge in OMF was investigated (Mahini and Ronagh. 2007). In this paper, three reinforced concrete frame modules of OMF, IMF and IMF with carbon fiber reinforced were tested under cyclic loading. The test results were evaluated for the seismic performance in terms of strength, ductility and energy dissipation.

2. TEST

2.1. Experimental Program

The generic moment frame modules were designed according to seismic provision of KBC 2009 and divided into OMF and IMF. The modules were a portal frame of a half scale and consisted of beam length of 3500mm and column length of 1900mm. Holes which matches floor patterns were placed in the foundation of specimens to fix the specimens on the strong floor. Plate and anchor bolts for lateral loading were installed at panel zone in beam-to-column connection before concrete was casted, and the anchor bolts shall be connected with the head of actuator. The specimens were divided into three types:

OMF, IMF and IMF strengthened with carbon fiber reinforced polymer (CFRP). OMF and IMF have different stirrup space. In OMF, the hoops were installed with even distance of 175mm through the column and panel zone as shown in Fig. 1(d). The stirrups are open U-shaped with equal spaces as shown in Fig. 1(b) and (c). In IMF specimen, stirrups at the panel zone and the bottom and top of the column are spaced with smaller spacing than other parts of frame as shown in Fig. 2(a). All hoops and stirrups are closed shape with seismic hooks. Detailing of specimens is shown in Figs. 1 and 2. Deformed bars with a diameter of 10mm (D10) and the yield strength of 300MPa were used as a longitudinal reinforcement in OMF. The reinforcement with a diameter of 10mm (HD10) and the yield strength of 400MPa were used in IMF. The stirrups with a diameter of 6mm were used in both test modules.
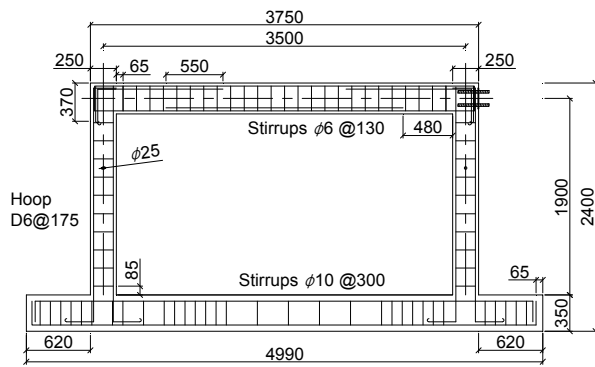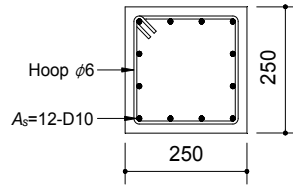
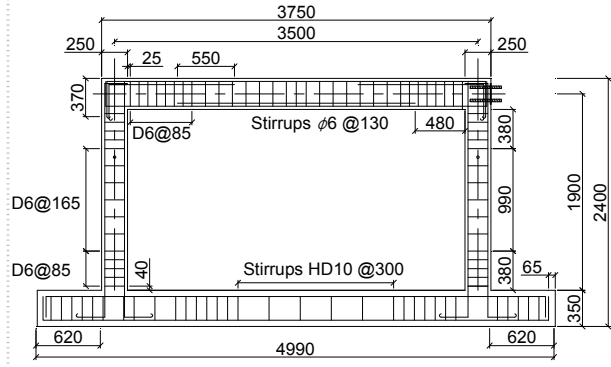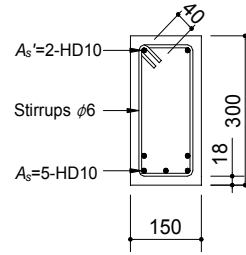**(a)** Detail of reinforcement
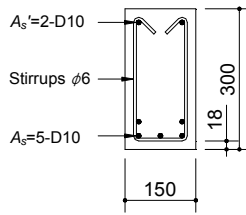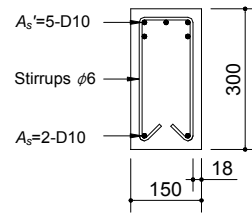
(b) Center of beam   **(c)** End of beam
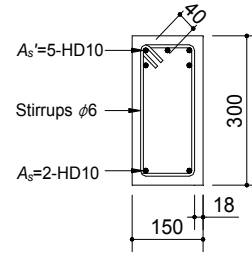
(d) Detail of column

Figure 1. Detail of OMF specimen
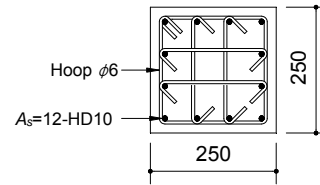
**(a)** Detail of reinforcement

(b) Center of beam   **(c)** End of beam

(d) Detail of column

Figure 2. Detail of IMF specimen

Fig. 3 shows an IMF specimen strengthened with CFRP at the bottom of column. The specimen were made according to the following order; grinding of concrete surfaces, primer coating, epoxy putty, and attaching carbon fiber sheets. CFRP were bonded from bottom of column to 500mm by three times overlapping. The specified concrete strength was 24MPa and ready mixed concrete using ordinary Portland cement, and maximum size of coarse aggregate was 20mm. Mixing proportion of concrete is shown in Table 1, and the result of slump test was 150mm. The compressive strength of concrete at 7 days and 28 days was measured using standard concrete cylinder of a diameter of 100mm and a height of 200mm based on Korean Industrial Standards.
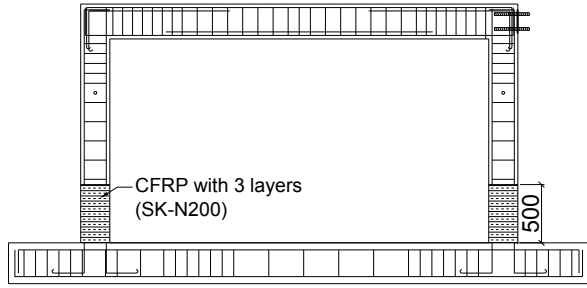
Figure 3. Detail of IMF with CFRP

Table 1. Design of Mixed Concrete

| Designing strength		24 MPa				
WC (%)	S/A (%)	Unit quantity of material (kg/m^3)				
		W	C	S	G	Admixture
47.9	47.6	180	376	811	904	2.63

2.2. Material Test

The test of compressive strength of the standard concrete cylinders was carried out using swivel to prevent the eccentric loading. Longitudinal deformation was measured by two linear variable differential transformers (LVDTs), and load was measured by loadcell mounted on UTM. The tensile test of reinforcement was also carried out according to the KS B 0801 of Korea Industrial Standards. Longitudinal deformation was measured by strain gauges attached on both surfaces of coupon and extensometer. The result of material test is shown in Table 2. Stress-strain curves of reinforcement and concrete are shown in Figs. 4 and 5. The compressive strength of concrete at 7 days and 28 days were 20.9MPa and 38.6MPa, respectively. The tested yield strength and tensile strengths of rebar (D10) were 329.0MPa and 518.5MPa, and those of rebar (HD10) were 411.1MPa and 616.1MPa, respectively.

Table 2. Result of Material Test

Material Test		Strength (MPa)			Average strength (MPa)
		1st	2nd	3rd	
strength of concrete at 7 day		20.6	21.1	20.9	20.9
strength of concrete at 28 day		39.8	34.4	41.2	38.6
D10	Yield strength(f_y)	329.7	331.1	326.2	329.0
	Ultimate strength(f_u)	517.6	518.5	519.3	518.5
HD10	Yield strength(f_y)	401.8	425.0	406.5	411.1
	Ultimate strength(f_u)	605.8	632.1	610.4	616.1
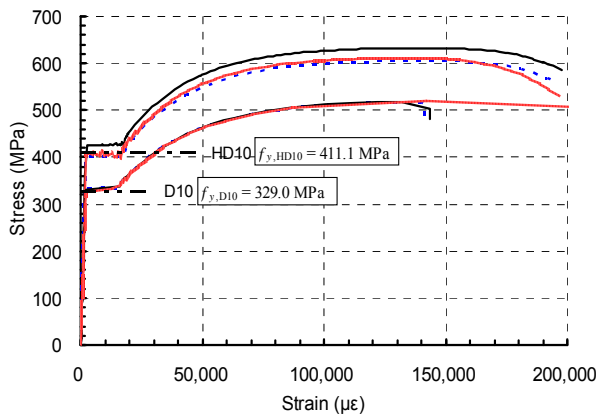
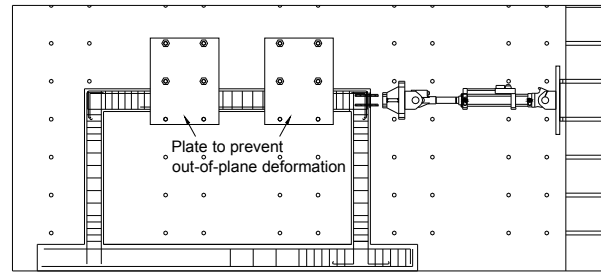**Figure 4.** Stress-strain curves of reinforcement
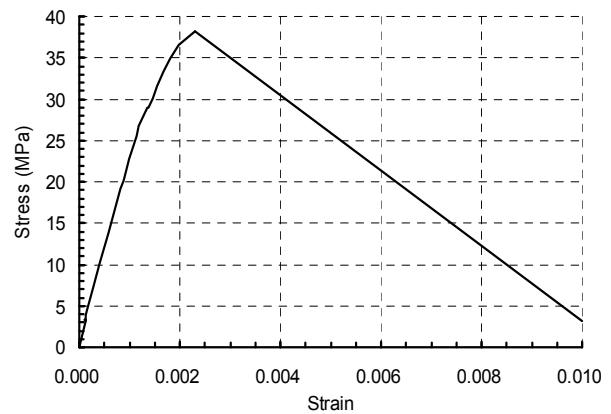
Figure 5. Stress-strain curves of concrete cylinder

The mechanical properties of CFRP of SK-N200 by the test reports are shown in Table 3. The bond strength of concrete of SK primer to attach the CFRP was 2.5MPa, and the bond strength and compressive strength of epoxy putty were 2MPa and 35MPa.

Table 3. Mechanical Properties of CFRP

Weight of Fiber	Specific Gravity of Fiber	Thickness of Design	Tensile Strength
200 g/m^2	1.8 g/cm^2	0.111 mm	390 N/mm
Design Strength	Tensile Modulus	Design Modulus	Strain at Failure
3,500 MPa	25,900 N/mm	2.35×10^5 MPa	1.5 %

The specimens were set up as illustrated in Figs. 6 and 7. The foundation of specimen was fixed by threaded bolts with a diameter of 42mm at the holes of strong floor. The four plates to prevent out-of-plane deformation were installed at two positions. Teflon which has a very low coefficient of friction, close to 0, was inserted between the plate and side of beam to reduce the friction.
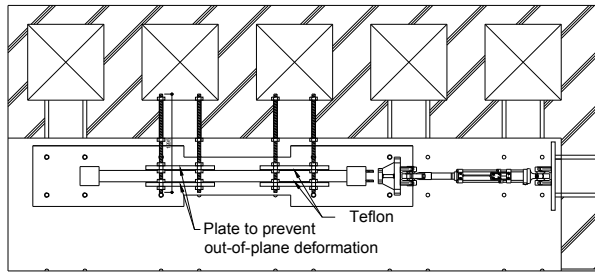

Figure 6. Floor plan of setup   **Figure 7.** Front view of setup

2.3. Loading and Measurement

The specimens were subjected to cyclic loading according to ACI 374.1-05 and cycles shall be predetermined drift ratios as defined in the following three steps.

(1) Three fully reversed cycles shall be applied at each drift ratio.
(2) The initial drift ratio shall be within the essentially linear elastic response range for the module. Subsequent drift ratios shall be to values not less than one and one-quarter times, and not more than one and one-half times, the previous drift ratio.
(3) Testing shall continue with gradually increasing drift ratios until the drift ratio equals or exceeds 0.035.

Based on the above three steps, actuator was first pushed and pulled to drift ratio of 0.5% (displacement of 9.5mm). Since then the drift ratio was gradually increased to 8% (displacement of 152.0mm). The actuator with maximum capacity of 500kN and stroke length of 500mm was used to apply cyclic loading using a displacement-control approach. Fig. 9 shows the location of sensors attached. The lateral displacement using LVDT mounted on the actuator was measured at the loading position. Additional two wire LVDTs with 500mm stroke were installed at the opposite loading position. The lateral displacement can be measured lateral displacement at three positions, simultaneously. In order to measure the slippage of the foundation, an LVDT with 20mm stroke was installed at the left side of the base and monitored. To measure the strain of rebar, embedded strain gauges were attached at both ends of beam and column, and polyurethane coating and water-resistant adhesive were used. To measure the plastic rotation, the crack gages were installed at extreme surfaces of a tension and a compression of both ends of beam and bottom of column as shown in Fig. 9. The crack gauges were installed with the distance of 300mm on the beam and 250mm on the column. Because the stroke of crack gauge was +-5mm, loading was temporarily stopped on the verge of exceeding the stroke and the crack gauge was reinstalled, and then repeated loading and measured until the end of the test.
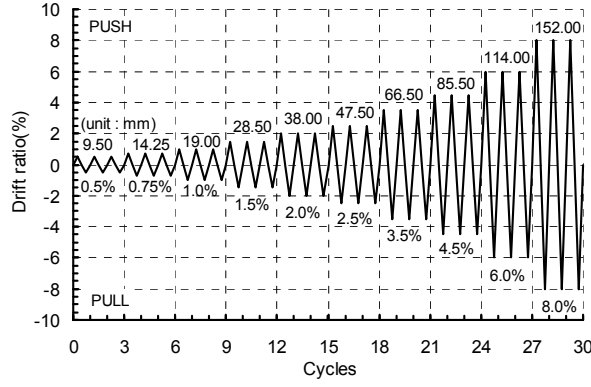
Figure 8. Loading history
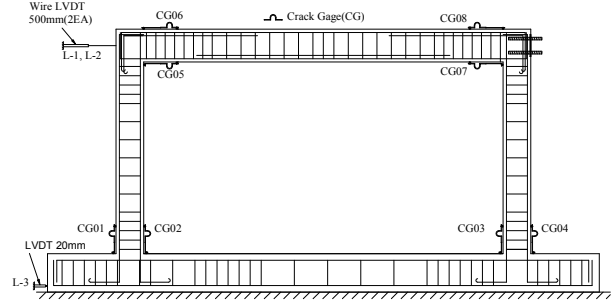
Figure 9. Sensor attached

Curvature at the bottom of column was determined through Fig. 10 and an equation (2.1) to (2.5). The measuring depth (h_c) between measuring points of a tension side and a compression side the bottom of column was determined by adding width of column and height (10mm×2) of fixing jig of crack gauge. The length ℓ_1 and ℓ_2 are the initial length of crack gauge attached at the ends of column. The change $\Delta\ell_1$ and $\Delta\ell_2$ are the displacement measured by crack gauge. The strain ε_1 and ε_2 are the strains of a tension and a compression side at the bottom of column, respectively. The average curvature ϕ_c along the length ℓ_1 is obtained by the Equation (2.3). The rotation angle θ_c is calculated by the Equation (2.4), which includes the elastic rotation $\theta_{e,c}$ and plastic rotation $\theta_{p,c}$.
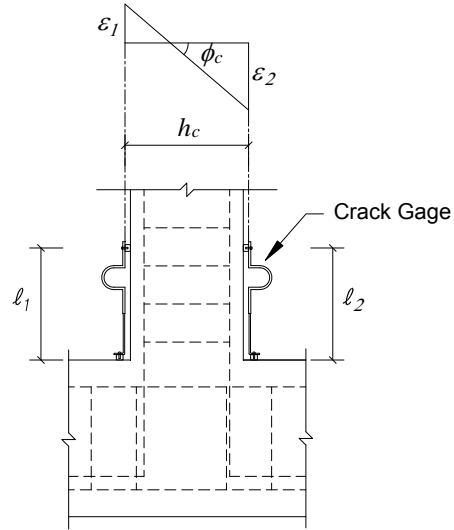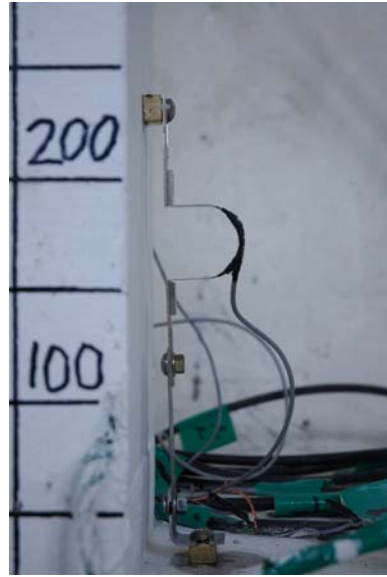
Figure 10. Curvature measurement using crack gages at the bottom of column

$$\varepsilon_1 = \Delta\ell_1 / \ell_1 \tag{2.1}$$

$$\varepsilon_2 = \Delta\ell_2 / \ell_2 \tag{2.2}$$

$$\phi_c = \frac{\varepsilon_1 - \varepsilon_2}{h_c} \tag{2.3}$$

$$\theta_c = \phi_c(\ell_1 \text{ or } \ell_2) \tag{2.4}$$

$$\theta_{p,c} = \theta_c - \theta_{e,c} \tag{2.5}$$

3. TEST RESULT AND ANALYSIS

3.1. Load-Displacement Curve and Dissipated Energy

Lateral load-displacement curves of the three specimens are shown in Figs. 11 ~ 14. Lateral load and displacement were measured by loadcell and LVDT mounted on the actuator. Pushing the frame was expressed as the positive direction (+), and pulling was the negative direction (-). In lateral load-displacement curves, stiffness and strength were decreased in the same drift ratio when three fully reversed cycles were applied progressively. Pinching tended to appear more clearly in the ordinary moment frame. In Fig. 11, the maximum load (L_{peak}) of OMF was 80.92kN in positive direction and -61.61kN in negative direction. Dissipated energy until first cycle of 6.0% drift ratio maintaining maximum load of 75% ($L_{0.75\%peak}$) was 61.27kN·m. In Fig. 12, the maximum load of IMF was 87.39kN and -69.21kN. The maximum load was increased by 8% and 12%, when compared to OMF. Dissipated energy until first cycle of 6.0% drift ratio was 71.29kN·m and increased by 16%. The maximum load of IMF strengthened with CFRP was 88.27kN and -69.59kN as shown in Fig. 13. Dissipated energy until second cycle of 4.5% drift ratio was 53.39kN·m. In Table 4, the maximum loads of IMF strengthened with CFRP were increased by 10%, but the dissipated energy was decreased. Fig. 14 shows the accumulative energy dissipation capacity of each specimen during the step of loading until the end of test. According to this figure, all three specimens appear similar in term of energy dissipation capacity until 2.5% drift ratio, since then dissipation capacity of IMF and IMF with CFRP can be found to appear larger gradually. However it was found that the IMF reinforced with CFRP does not differ greatly depending on the drift ratio until the end of test over the IMF frame as expected. Overall accumulated dissipated energy until $L_{0.75\%peak}$ after peak load of IMF with CFRP was lower than that of other modules. From this point, IMF with CFRP showed the effect of strength enhancement but less ductile behavior was obtained due to the stress concentration in the panel zone.
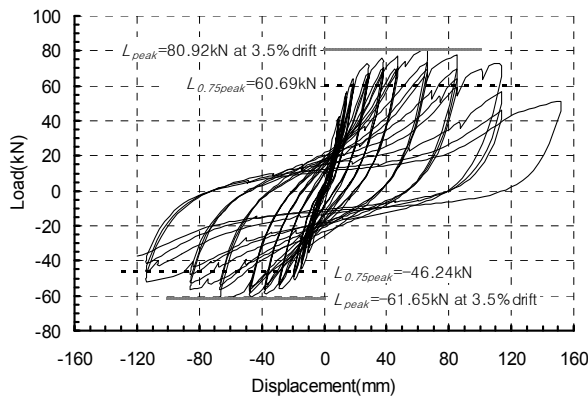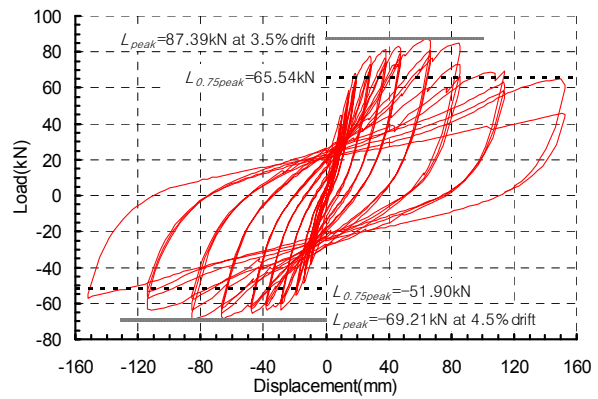

Figure 11. Hysteric curve of OMF
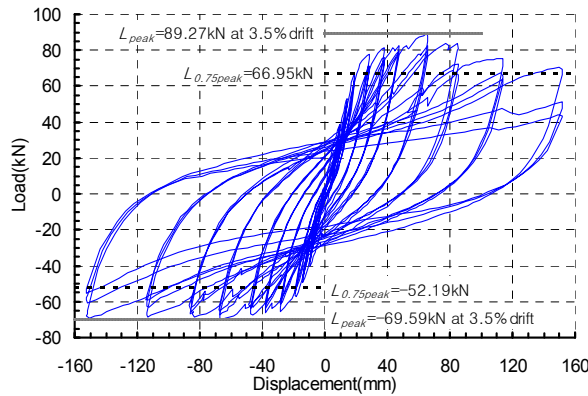

Figure 12. Hysteric curve of IMF

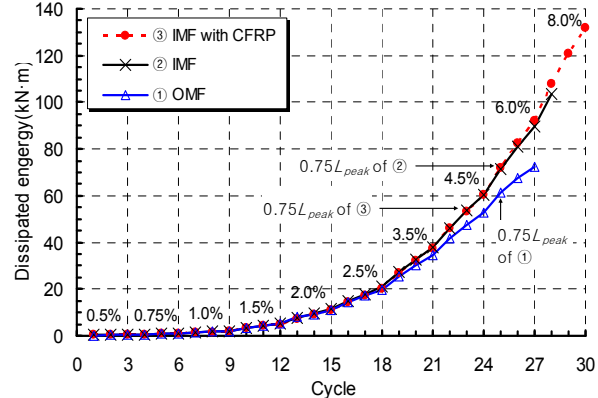**Figure 13.** Hysteric curve of IMF with CFRP

Figure 14. Energy dissipation capacity

Table 4. Test Result Summary

| Specimen	Maximum resistance (kN)		Ratio of maximum resistance (%)		Energy dissipation	
	(+) direction	(-) direction	(+) direction	(-) direction	(kN·m)	Increment (%)
OMF	80.9	-64.7	1.00	1.00	61.3	-
IMF	87.4	-69.2	1.08	1.12	71.3	+16
IMF with CFRP	89.3	-69.6	1.10	1.13	53.4	-13
Dissipated energy is calculated by step up to maintain $L_{0.75\%peak}$						

3.2. Plastic Rotation

Figs. 15 ~ 17 show the load versus plastic rotation suggested by Pan et al. (1989) at the bottom of left column. The plastic rotation was calculated by excluding elastic rotation from total rotation. The elastic rotation is defined as a rotation angle at the 2/3 of maximum load. The plastic rotations maintaining the maximum load of 75% were 0.0597 rad and –0.0374 rad in OMF. In IMF and IMF with CFRP, the plastic rotation were 0.056 rad, -0.0377 rad, 0.0338 rad, and –0.0284 rad, respectively. The plastic rotations in positive direction tended to be larger than in negative direction. The plastic rotations were compared to acceptance criteria for nonlinear procedure of reinforced concrete frames according to KBC2009 and FEMA356. In case of column with nonconforming transverse reinforcement, axial force ratio of less than 0.1 and shear force ratio of less than 0.25, acceptance criteria of plastic rotation is 0.006 rad. The plastic rotations are considerably higher than acceptance criteria. The plastic rotation of each specimen might be measured higher than the actual size of the specimen because a 1/2 scale modules were produced and carried out.
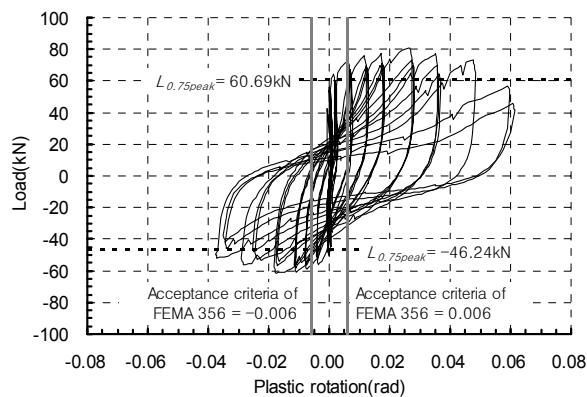
Figure 15. Hysteric curve of OMF
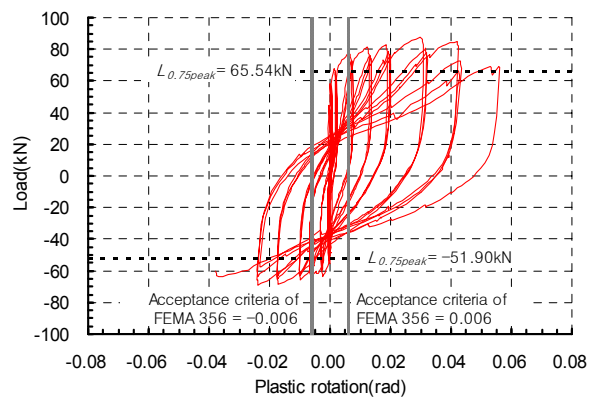
Figure 16. Hysteric curve of IMF
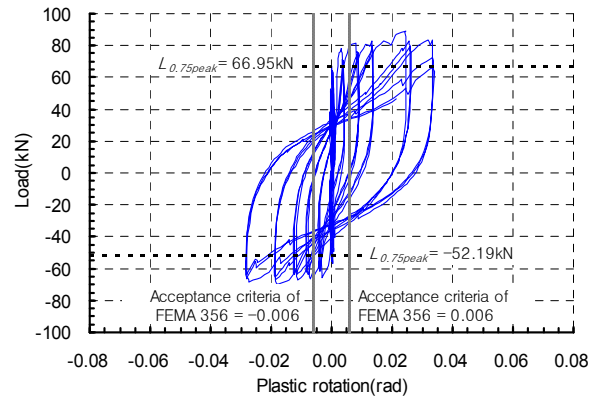

Figure 17. Hysteric curve of IMF with CFRP

3.3. Fracture Modes

In OMF specimen, it can be observed that cracks began to grow from the bottom of the beam which has small amount of rebar at 1.00% drift ratio. And in the 2.0% drift ratio, opening crack of more than 5mm was observed. In column, the spalling failure of cover concrete occurred at the bottom and rebar was exposed at 4.5% drift ratio. In IMF specimen, crack and opening phenomenon is not significantly different from OMF specimen. Because of the narrow stirrup spacing, however, spalling of cover concrete was found to appear at a lower load than OMF specimen. The IMF specimen reinforced with CFRP was very similar to the other two specimens during 2.5% drift ratio. Crack formation was delayed by CFRP and the opening phenomenon intensively was started at 3.5% drift ratio. The surface of CFRP began to tear at 4.5% drift ratio. In the panel zone, concrete spalling failure occurred by showing a typical shear failure pattern with diagonal cracking.
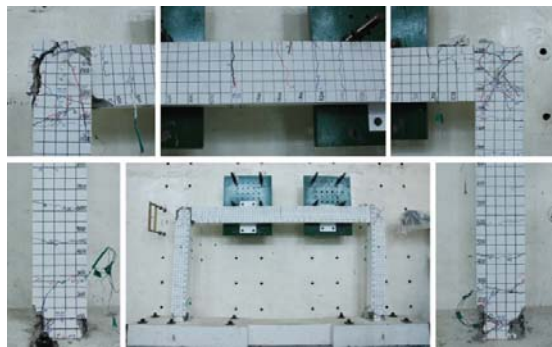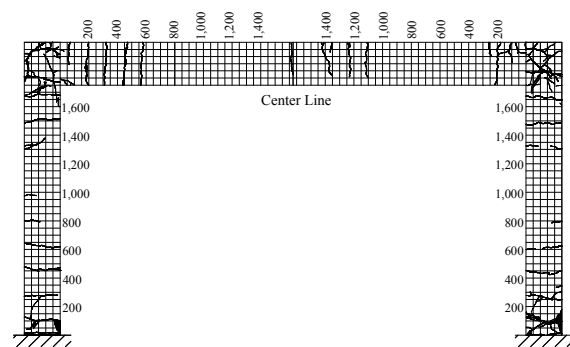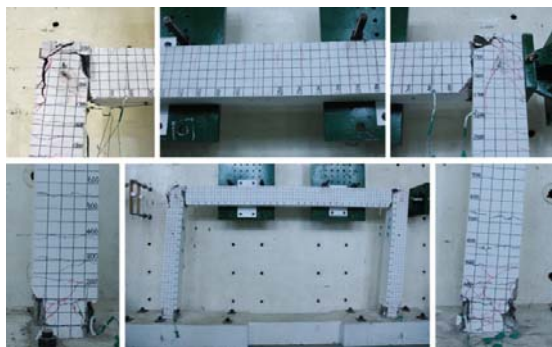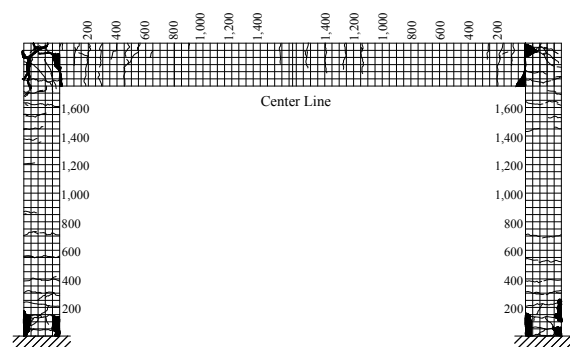

(a) Failure mode   **(b)** Crack pattern

Figure 18. Test result of OMF

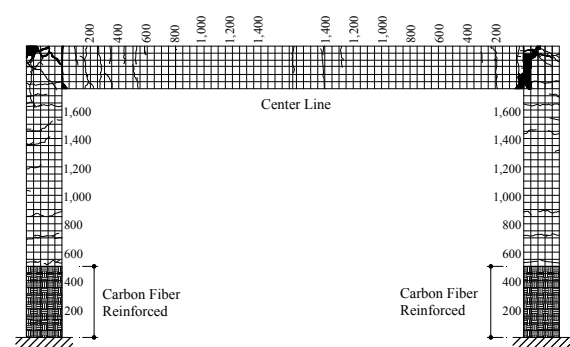
(a) Failure mode   **(b)** Crack pattern

Figure 19. Test result of IMF

(a) Failure mode   **(b)** Crack pattern

Figure 20. Test result of IMF with CFRP

4. CONCLUSIONS

In this paper, an experiment of the moment frames, which were designed according to earthquake resistant design, was conducted. The three specimens, OMF, IMF, and IMF strengthened with carbon fiber sheets were tested, and the results of behavior were analyzed. The following conclusions were drawn based on the results of the cyclic tests.
.
1) The maximum loads of IMF and IMF strengthened with carbon fiber sheets were increased by 10% compared to that of OMF.
2) Dissipated energy of IMF specimen was increased by 16% compared to that of OMF, but IMF strengthened with carbon fiber sheets was decreased by 13%. It means that strengthening the bottom of columns induces more stress concentration and large deformation at the top beam-column connections which results in less ductility.
3) All specimens were satisfied with acceptance criteria for criteria for the third cycle between peak drift ratios of 3.5% in ACI 374.

REFERENCES

Han, S.W. and Jee, N.Y. (2005). Seismic behaviors of columns in ordinary and intermediate moment resisting concrete frames. *Engineering Structures*. **27**, 951-962.

Kang, T.H.-K., Ha, K.S. and Choi, D.U. (2010). Bar pullout tests and seismic tests of small-headed bars in beam-column joints. *ACI Structural Journal* **107:1,** 32-42.

Pan, A. and Moehle, J. P. (1989). Lateral displacement ductility of reinforced concrete, *ACI Structural Journal*, **86:3**, 250-258.

ACI Committee 318. (2011). Building Code Requirements for Structural Concrete (ACI 318M-11) and Commentary. American Concrete Institute. Farmington Hills, MI, U.S.A.

ACI Committee 374. (2005). Acceptance Criteria for Moment Frames Based on Structural Testing and Commentary (ACI 374.1-05), American Concrete Institute, Farmington Hills, MI, U.S.A.

Architectural Institute of Korea. (2009). Korean Building Code and Commentary. Seoul. Rep. of Korea.

Mahini, S.S. and Ronagh, H.R. (2007). Seismic upgrading of existing RC ordinary moment resisting frames using FRPS. *Asia-Pacific Conference on FRP in Structures*. 221-226.